Citation: Chen, B. and Wang, K. and El-Mowafy, A. and Yang, X. 2024. Real-Time GNSS satellite SISRE and its integrity for LEO satellite POD. In Proceedings of 2024 International Technical Meeting of The Institute of Navigation, 23 - 25 Jan 2024, Long Beach, California.

PEER REVIEWED

Real-Time GNSS satellite SISRE and its integrity for LEO satellite Precise Orbit Determination

Beixi Chen, *National Time Service Center, Chinese Academy of Sciences, Xi'an, China; University of Chinese Academy of Sciences, Beijing, China; Key Laboratory of Time Reference and Applications, Chinese Academy of Sciences*
Kan Wang, *National Time Service Center, Chinese Academy of Sciences, Xi'an, China; University of Chinese Academy of Sciences, Beijing, China; Key Laboratory of Time Reference and Applications, Chinese Academy of Sciences*
Ahmed El-Mowafy, *School of Earth and Planetary Sciences, Curtin University, Perth, Australia*
Xuhai Yang, *National Time Service Center, Chinese Academy of Sciences, Xi'an, China; University of Chinese Academy of Sciences, Beijing, China; Key Laboratory of Time Reference and Applications, Chinese Academy of Sciences*

Biographies

Beixi Chen is a Ph.D. candidate at the National Time Service Center, Chinese Academy of Sciences. His research interests include LEO-augmented GNSS positioning, LEO/GNSS satellite products and their integrity.
Kan Wang is a Professor at the National Time Service Center, Chinese Academy of Sciences. She received her PhD in GNSS advanced modeling from ETH Zurich in 2016. Her research interests include high-precision GNSS positioning, LEO-augmented PNT service, LEO satellite POD and clock determination, and integrity monitoring.
Ahmed El-Mowafy is a Professor of Positioning and Navigation, leader of the GNSS research group, and Director of Graduate Research, School of Earth and Planetary Sciences, Curtin University, Australia. He obtained his Ph.D. from the University of Calgary, Canada, in 1995. He has more than 220 publications in precise positioning and navigation using GNSS, quality control, integrity monitoring and estimation theory.
Xuhai Yang is a Professor at the National Time Service Center, Chinese Academy of Sciences. Since 2007, he has served as the director of the research department of high-precision time transfer and precise orbit determination. His research interests include high-precision time transfer, VLBI, and orbit determination.

Abstract

The real-time Global Navigation Satellite System (GNSS) precise orbital and clock products are essential prerequisites for the Positioning, Navigation, and Timing (PNT) services and have been assessed in various studies. Compared to the precision of the orbital and clock products, their combined effect expressed in Signal-In-Space Ranging Error (SISRE) is of higher concern for positioning users. As a special user of the GNSS, the Low Earth Orbit (LEO) satellites need high-precision real-time GNSS products for their Precise Orbit Determination (POD) and clock determination in real time, which enables the future LEO-augmented GNSS PNT service. This study performs a comprehensive analysis of the real-time GNSS products from five different analysis centers, including analysis of their continuity, accuracy of their orbits, precision of their clocks, and their SISREs for LEO satellites at different altitudes. Using the tested products, the LEO POD was also performed to verify the correlation between the quality of the GNSS products and the accuracy of the LEO POD. Furthermore, to assess the integrity of real-time GNSS products, the overbounding standard deviations and mean values of the combined clock and orbital errors were computed and compared for different institutions. It was found that the GPS and Galileo SISRE range from a few centimeters to around 8 cm, while the SISRE of the Beidou Satellite Navigation System (BDS) Medium Earth Orbit (MEO) is a bit worse, i.e., around 1-2 dm. It has been demonstrated that there exists a positive correlation between the SISRE and user altitude, which implies a higher bias introduced to LEO satellites than ground users. The overbounding standard deviations and mean values of the GPS and Galileo products are all within 1 dm, whereas for BDS they are about 1-2 dm. Among the tested products, the smallest SISRE and overbounding values were delivered by the National Centre for Space Studies (CNES) in France for GPS and Galileo, while the GNSS Research Center of Wuhan University (WHU) provided the best accuracy and integrity for the BDS MEO products.

Keywords: GNSS; LEO; Signal-In-Space Range Error (SISRE); Integrity

 https://doi.org/10.33012/2024.19488

1. INTRODUCTION

In recent years, Low Earth Orbit (LEO) satellites are frequently discussed to serve as an augmentation to Global Navigation Satellite Systems (GNSSs) to enable better performances of the Positioning, Navigation, and Timing (PNT) services (Reid et al., 2018). Benefiting from the much lower orbital heights of LEO satellites (at a few hundred kilometers to about 1500 km) than the GNSS satellites flying at Medium Earth Orbits (MEOs)(Montenbruck & Gill, 2000), users on the ground can enjoy numerous advantages during positioning and timing. These include but are not limited to: 1) a higher number of visible satellites and a better satellite geometry in areas like urban canyons or forests (Lawrence et al., 2017); 2) a much stronger signal strength than the GNSS satellites with a better anti-jamming capability (GPS World Staff, 2017); 3) a fast geometry change and as a result, a significantly shortened convergence time in the Precise Point Positioning (PPP) and PPP – Real-Time Kinematic (PPP-RTK) positioning (Ge et al., 2018; Li et al., 2018a; Wang et al., 2022); 4) a lower cost in general compared to the GNSS satellites.

To demonstrate the above-mentioned benefits of LEO-augmented GNSS positioning services, lots of studies have been performed based on simulated LEO satellite constellations and signals. As LEO satellites transmitting GNSS-like navigation signals as carrier-phase and pseudo-range measurements are about to become true in the near future (Yang, 2019; Michalak et al., 2021; Reid et al., 2022; Wang et al., 2022), real-time high-accuracy LEO satellite orbital and clock products are important preconditions to realize the LEO-augmented PPP on the ground. In the past decades, various studies were performed to achieve cm-level accuracy for LEO satellite POD. Making use of high-quality GNSS measurements collected onboard LEO satellites and appropriate dynamic models, mature techniques were developed to obtain high-quality orbital and clock products in near-real-time or real-time in the reduced-dynamic mode (Montenbruck et al., 2013; Hauschild et al., 2016, 2022; Allahvirdi-Zadeh et al., 2021a). In addition to the different computational power onboard LEO satellite or on the ground, and the differences between the GNSS data quality and dynamic models used for the POD in diverse studies, a major factor for the accuracy of the LEO satellite products is the accuracy of the used real-time GNSS satellite products. The LEO satellite orbital accuracy, as an example, could vary from a few centimeters using high-quality real-time GNSS products from IGS analysis centers to the dm-level when using broadcast ephemeris.

For processing on ground, diverse choices of real-time GNSS products exist. Studies have been performed to analyze and compare the accuracy of real-time GNSS satellite products from various analysis centers (Li et al., 2022; Yu et al., 2022). The analysis is performed mostly separately for satellite orbits and clocks, and aims to serve ground users. However, the Signal-In-Space Range Errors (SISREs), which describe the averaged projection of the combined satellite orbital and clock errors to the Earth, are of higher concern for users. As an extension to the anaylsis of the clock and orbital accuracy separately, in this study, the SISRE of the up-to-date real-time multi-GNSS satellite products from five different analysis centers are analyzed and compared for LEO satellites at 500, 1000, and 1500 km heights. Due to the much higher altitudes of LEO satellites than users on the ground, the projection coefficients of the GNSS satellite SISRE to LEO satellites vary from those of the ground users. The role of the radial orbital errors decreases at the expense of increasing the role of the along-track and cross-track components. As a comparison to the SISRE of the GNSS satellites to LEO satellites, the SISRE of the real-time GNSS streams is also given for ground users.

In addition to the SISRE, the integrity of real-time GNSS satellite products is essential for integrity monitoring of the LEO satellite POD and clock determination (Wang et al., 2021; 2022). As such, this contribution also provides an analysis of the integrity of the investigated real-time GNSS products. The continuities of the received streams are investigated. The overbounding standard deviations and mean values (bias) of the combined GNSS satellite orbital and clock errors are computed for different constellations using the Stanford two-step method (Blanch et al., 2019). This leads to the calculation of the overbounding values for their SISREs to LEO satellites and ground users.

The paper starts with introducing the real-time GNSS products used. It is followed by the processing strategies employed for analysis of the GNSS satellite clocks, orbits, and SISREs to the LEO satellites and ground users. A short summary to calculating the overbounding standard deviations and mean values using the two-step method is given afterward. It is followed by an analysis and comparison of the GPS, Galileo, and BDS satellite products from five analysis centers, including their continuities, orbital accuracies, clock precision, and the SISREs for LEO satellites (as the users) at different altitudes, and ground users. A brief discussion on LEO POD using these investigated real-time products is then given. The overbounding values of the combined satellite orbital and clock errors are computed and demonstrated next. The conclusion is given at the end of the paper.

2. PROCESSING STRATEGIES

The processing is split into three parts. The first part analyzes the multi-GNSS real-time satellite orbital accuracy and clock precision using the products provided by five analysis centers, i.e., the National Centre for Space Studies (CNES) in France (Kazmierski et al., 2018), the GeoForschungsZentrum (GFZ) (Männel et al., 2020), the GMV Aerospace and Defense (GMV, 2023), the GNSS Research Center of Wuhan University (WHU) (Guo et al., 2018), and the Innovation Academy for Precision Measurement Science and Technology, Chinese Academy of Sciences (CAS) (Ding et al., 2018). The real-time GNSS products are compared with the Multi-GNSS Experiment (MGEX) final products from the Center for Orbit Determination in Europe (CODE) (Villiger et al., 2019; Schaer et al., 2021) (COM) for accuracy and precision analysis.

In the second part, the SISREs of the above-mentioned real-time products are calculated for LEO satellites at different altitudes and for ground users for their comparison at these two application levels. The third part attempts to calculate the overbounding standard deviations and the nominal biases, i.e. mean values, of the combined GNSS satellite orbital and clock errors.

2.1. Real-time GNSS satellite orbits and clocks

The different real-time orbital products are compared with the COM final orbits in the radial (R), along-track (T) and cross-track (A) directions in a straightforward manner:

$$\Delta r^s_{\mathrm{RT,RTA}} = R_{\mathrm{ECEF2RTA}} \cdot \left(r^s_{\mathrm{ECEF,RT}} - r^s_{\mathrm{ECEF,COM}}\right) \tag{1}$$

where $r^s_{\mathrm{ECEF,RT}}$ and $r^s_{\mathrm{ECEF,COM}}$ represents the real-time and COM final orbital vector of GNSS satellite s, respectively, computed in the Earth-Centered Earth-Fixed (ECEF) system, more specifically, under IGS20. R_{ECEF2RTA} is the rotation matrix transforming the ECEF orbital differences into the RTA orbital system. $\Delta r^s_{\mathrm{RT,RTA}}$ is the real-time orbital error vector of GNSS satellite s in the RTA directions.

To compare the real-time and the COM final clock products, re-referencing needs to be performed first considering the different time references between the real-time and COM final products. In this study, the epoch-wise mean differences between the two products of a selected subset of clocks in each GNSS constellation are used to re-reference the real-time clock products for the corresponding constellation. The re-referenced clock $d\tilde{t}^s_{\mathrm{RT}}$ can be expressed as:

$$d\tilde{t}^s_{\mathrm{RT}} = dt^s_{\mathrm{RT}} - \frac{\sum_{i=1}^{n}\left(dt^i_{\mathrm{RT}} - dt^i_{\mathrm{COM}}\right)}{n} \tag{2}$$

where dt^i_{RT} and dt^i_{COM} denotes the original real-time clock bias and COM final clock bias of GNSS satellite i, respectively. n is the number of selected clocks used for re-referencing in the corresponding constellation. The clock error $\Delta\tilde{t}^s_{\mathrm{RT}}$, in this case, can be obtained by differencing the re-referenced real-time clock bias and the COM final clock bias:

$$\Delta\tilde{t}^s_{\mathrm{RT}} = d\tilde{t}^s_{\mathrm{RT}} - dt^s_{\mathrm{COM}} \tag{3}$$

The orbital and clock errors are calculated for each epoch and for each satellite. The average Root Mean Square (RMS) of the orbital errors ($\bar{\sigma}^s_d$) and average Standard Deviation (STD) of the clock errors ($\bar{\sigma}^s_{dt}$) are computed as follows:

$$\bar{\sigma}^s_d = \sqrt{\frac{\sum_{j=1}^{m}\left(\sigma^s_{d,k}\right)^2}{m}} \tag{4}$$

$$\bar{\sigma}^s_{dt} = \sqrt{\frac{\sum_{j=1}^{m}\left(\sigma^s_{dt,k}\right)^2}{m}} \tag{5}$$

where d denotes the direction of the orbits, which could be radial, along-track or cross-track directions. m denotes the number of days used for the analysis. $\sigma^s_{d,k}$ represents the daily RMS of the real-time orbital errors for GNSS satellite s in direction d on day k,

whereas $\sigma^s_{dt,k}$ represents the daily STD of the real-time clock errors for GNSS satellite s on day k. Note that by calculating each daily RMS or STD, a threshold of mean value plus/minus 4.42 times of the standard deviation was used for outlier detection and exclusion.

2.2. GNSS satellite SISRE to LEO satellites

The SISRE of GNSS satellites can be computed as follows (Montenbruck et al., 2018):

$$\sigma^s_{\mathrm{SISRE}} = \sqrt{(\sigma^s_{\mathrm{R}\Delta t})^2 + \omega^2_{\mathrm{TA}}((\sigma^s_{\mathrm{T}})^2 + (\sigma^s_{\mathrm{A}})^2)} \tag{6}$$

with

$$\sigma^s_{\mathrm{R}\Delta t} = \mathrm{RMS}\left(\omega_{\mathrm{R}} \times \Delta r^s_{\mathrm{RT,R}} - c \times \Delta \tilde{t}^s_{\mathrm{RT}}\right) \tag{7}$$

where $\Delta r^s_{\mathrm{RT,R}}$ denotes the radial real-time orbital error of GNSS satellite s. σ^s_{T} and σ^s_{A} denotes the RMS of the real-time along-track and cross-track orbital errors, respectively. c is the speed of light, and recall that $\Delta \tilde{t}^s_{\mathrm{RT}}$ is the real-time clock error of GNSS satellite s after removing its daily mean value. The projection coefficients ω_{R} and ω_{TA} are calculated according to Chen et al. (2013), which is dependent on the height of the GNSS satellites and the altitude of the user. In general, the nearer the GNSS satellites to the projection sphere, the larger are the contributions of the along-track and the cross-track components.

Assuming an Earth mean radius of 6371 km, and considering the average satellite orbital heights for GPS, Galileo and BDS MEO satellites in the test week of August 8-14, 2023, of about 20190, 23122 and 21535 km, respectively, the projection coefficients of the multi-constellation GNSS satellites to ground users (assumed at zero altitude) and LEO satellites at 500, 1000 and 1500 km are listed in Table 1.

Table 1

Projection coefficients of multi-constellation GNSS satellites to Earth and LEO satellites of different altitudes

Altitude (km)	GPS		Galileo		BDS (MEO)	
	ω_{R}	ω_{TA}	ω_{R}	ω_{TA}	ω_{R}	ω_{TA}
0	0.9792	0.1428	0.9832	0.1282	0.9812	0.1357
500	0.9758	0.1544	0.9805	0.1386	0.9782	0.1467
1000	0.9718	0.1660	0.9774	0.1490	0.9748	0.1578
1500	0.9678	0.1778	0.9742	0.1595	0.9709	0.1689

2.3. Overbounding values of the combined real-time orbital and clock errors

To have an insight into the impact of real-time GNSS orbital and clock errors on solution integrity, the overbounding standard deviations and mean values for the real-time along-track and cross-track orbital errors, and combined radial and clock errors are searched. Various methods exist for computing the overbounding values of an empirical distribution. Compared to the traditional paired overbounding method (Rife et al., 2006), the two-step method (Blanch et al., 2019) leads to a smaller overbounding mean value (i.e., nominal bias) and is thus used in this study.

With the overbounding standard deviations for the above-mentioned orbital and clock errors calculated, the overbounding standard deviations of the combined GNSS clock and orbital errors projected onto the LEO satellites (or Earth), denoted as $\breve{\sigma}^s_{\mathrm{SISRE}}$, can be expressed as (Heng et al., 2011; Wang et al., 2021):

$$\breve{\sigma}^s_{\mathrm{SISRE}} = \sqrt{(\breve{\sigma}^s_{\mathrm{R}\Delta t})^2 + \omega^2_{\mathrm{TA}}((\breve{\sigma}^s_{\mathrm{T}})^2 + (\breve{\sigma}^s_{\mathrm{A}})^2)} \tag{8}$$

where $\breve{\sigma}^s_{\mathrm{R}\Delta t}$ denotes the overbounding standard deviation of the term $\sigma^s_{\mathrm{R}\Delta t}$ (see Eq. (7)). $\breve{\sigma}^s_{\mathrm{T}}$ and $\breve{\sigma}^s_{\mathrm{A}}$ denote the overbounding standard deviations of the along-track and cross-track orbital errors, respectively.

Similarly, the overbounding mean value of the combined clock and orbital errors, denoted as $\breve{m}^s_{\mathrm{SISRE}}$, can be calculated as follows:

$$\breve{m}^s_{\mathrm{SISRE}} = \breve{m}^s_{\mathrm{R}\Delta t} + \omega_{\mathrm{TA}} \times (\breve{m}^s_{\mathrm{T}} + \breve{m}^s_{\mathrm{A}}) \tag{9}$$

where $\breve{m}^s_{\mathrm{R}\Delta t}$ denotes the overbounding mean value of the term $\left(\omega_{\mathrm{R}} \times \Delta r^s_{\mathrm{RT,R}} - c \times \Delta \tilde{t}^s_{\mathrm{RT}}\right)$ (see Eq. (7)). $\breve{m}^s_{\mathrm{T}}$ and $\breve{m}^s_{\mathrm{A}}$ denote the overbounding mean values of the along-track and cross-track orbital errors, respectively.

3. TEST RESULTS

As mentioned at the beginning of Section 2, the real-time GNSS satellite products from five different analysis centers, shortened as CNE, GFZ, GMV, WHU, CAS, are analyzed. Real-time streams are saved using the BNC software (Weber et al., 2007) for one week from August 8, 2023, at 7:43 to August 14, 2023, at 5:33 in the GPS Time (GPST). The sampling interval of clocks is 30 s, and the sampling interval of orbits is 5 min.

As a representative example, Figure 1 shows the continuity of the received GPS clock products during the test period. Small data gaps exist in all products, which could be attributed to diverse reasons including the instability of the internet connection. Table 2 gives an overview of the continuity of all constellations and products. It can be seen that the continuity of the GPS and Galileo products are very similar, while the received BDS products suffer from more data gaps.

Figure 1

Continuity of the received real-time GPS satellite clocks from five analysis centers

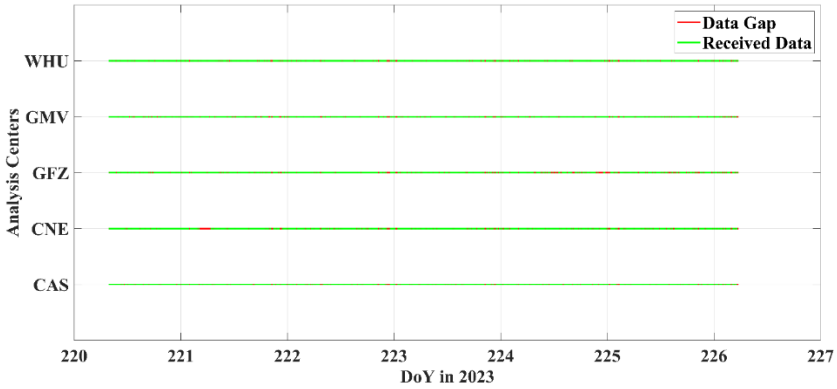

Table 2

The ratio between the number of available epochs and the number of epochs that were expected to be received for clock products from different analysis centers

Acs	Constellation		
	GAL	GPS	BDS
CAS	93.78%	93.81%	77.84%
CNE	91.60%	91.60%	--
GFZ	87.46%	87.46%	87.46%
GMV	92.29%	92.29%	--
WHU	94.04%	94.04%	78.39%

3.1. Accuracy of the real-time GNSS satellite orbits

To assess the accuracy and integrity of the combined GNSS satellite orbital and clock errors, the orbital and clock errors were first studied independently of the application thought. To this end, the accuracy of the real-time orbits is assessed as explained in Section 2.1. As shown in Figures 2-4, a 7-day average of the RMS is calculated for orbital errors in each direction and for each GPS, Galileo and BDS MEO satellite (see Eq. (4)) that could be used to determine LEO POD. In general, it can be observed that a rather good orbital accuracy can be achieved for GPS satellites in real-time, i.e., mostly within 5 cm in each direction. The Galileo orbital accuracy is slightly worse than that of the GPS satellites. It still remains below 5 cm in the radial and cross-track directions most of the time, but exhibits a bit worse behaviors in the along-track direction (see the green bars in Figure 3). The accuracy of the BDS MEO orbits is also assessed, which is generally worse than those of the GPS and Galileo satellites. PRNs not receiving real-time products or missing large periods of data are not illustrated with bars.

Figure 2

Accuracy of the real-time GPS orbital errors from different analysis centers. The abbreviations of the institution names were explained at the beginning of Section 2

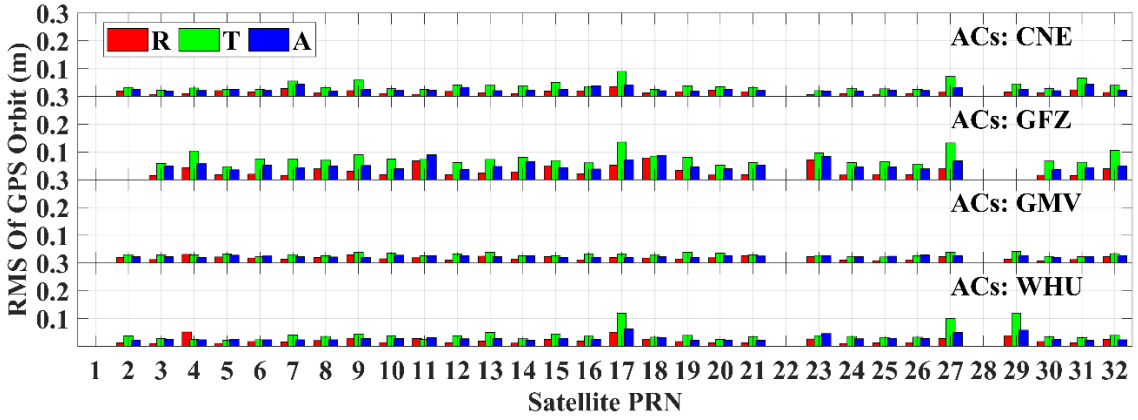

Figure 3

Accuracy of the real-time Galileo orbital errors from different analysis centers.

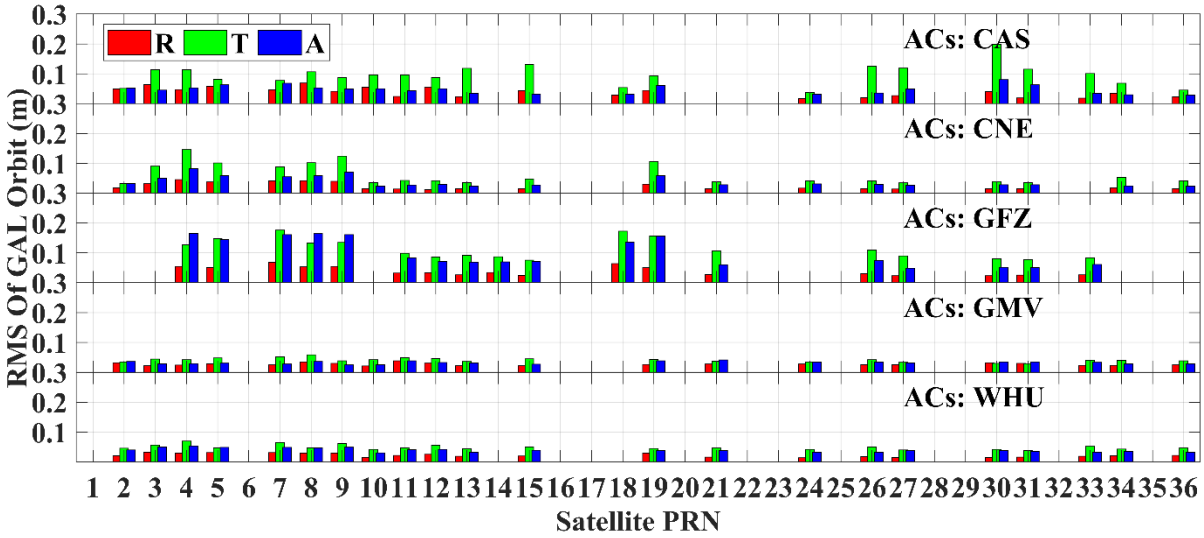

Figure 4

Accuracy of the real-time BDS (MEO) orbital errors from different analysis centers

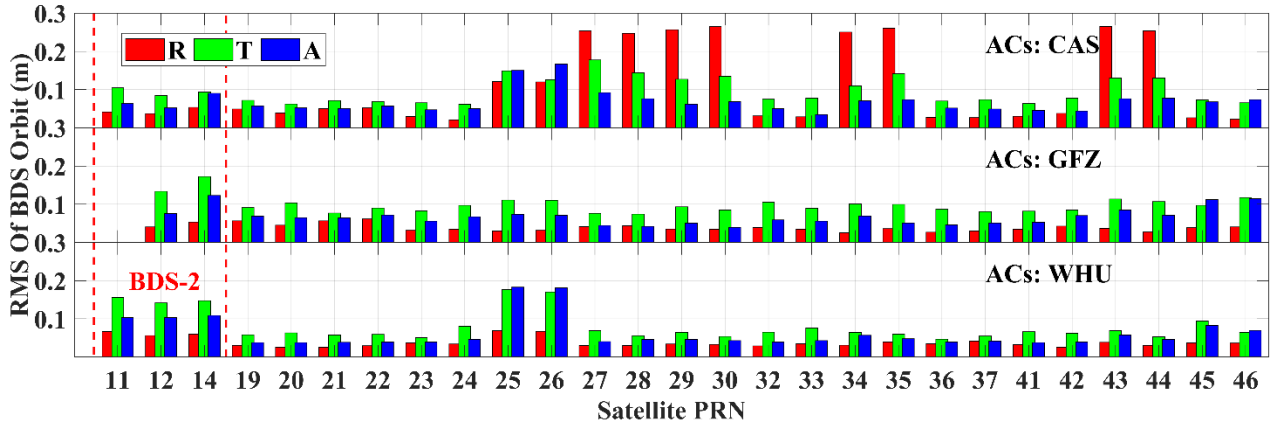

Taking the average for all satellites in each constellation, the real-time orbital accuracy is shown in Table 3 using the COM final products as the reference. It can be seen that during the test week, the GMV products exhibited the best accuracy for GPS and Galileo orbits, i.e., with a 3D RMSE below 5 cm. The WHU products showed the best behavior for BDS MEO satellite orbits, i.e., with a 3D RMSE of about 12 cm.

Table 3

RMS of the real-time orbital errors in the radial (σ_R), along-track (σ_T), cross-track (σ_A) and 3D (σ_{3D}) directions for GPS (G), Galileo (E) and BDS MEO (C) satellites

Acs	σ_R (m)			σ_T (m)			σ_A (m)			σ_{3D} (m)		
	G	E	C	G	E	C	G	E	C	G	E	C
CAS	/	0.0415	0.1465	/	0.1022	0.1030	/	0.0491	0.0746	/	0.1207	0.1940
CNE	0.0169	0.0256	/	0.0416	0.0715	/	0.0266	0.0427	/	0.0522	0.0871	/
GFZ	0.0360	0.0420	0.0397	0.0798	0.1176	0.1007	0.0545	0.1200	0.0706	0.1031	0.1665	0.1293
GMV	0.0190	0.0274	/	0.0312	0.0419	/	0.0245	0.0324	/	0.0440	0.0595	/
WHU	0.0234	0.0230	0.0407	0.0494	0.0495	0.0896	0.0315	0.0401	0.0744	0.0630	0.0678	0.1233

3.2. Accuracy of the real-time GNSS satellite clocks

The precision of GNSS satellite clocks plays a major role in the SISRE. Figures 5-7 illustrate the STD of the real-time satellite clocks for GPS, Galileo and BDS MEO satellites. It can be observed that the GPS and Galileo satellite clocks can nowadays mostly achieve a rather good precision of 0.1 to 0.2 ns, while the BDS MEO satellite clocks behave a little worse, i.e., mostly 0.2 to 0.3 ns. The BDS-3 MEO satellite clocks from WHU exhibit a good precision of 0.1 to 0.2 ns (see Figure 7), while its BDS-2 MEO satellite clocks behave worse.

Figure 5

Precision of the real-time GPS satellite clock errors from different analysis centers

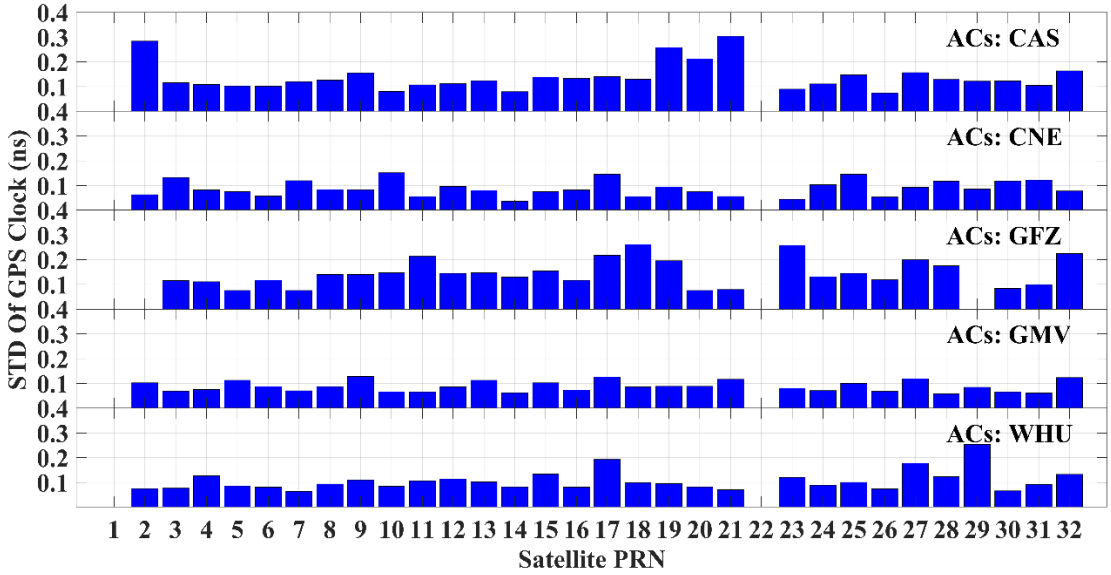

Figure 6

Precision of the real-time Galileo satellite clock errors from different analysis centers

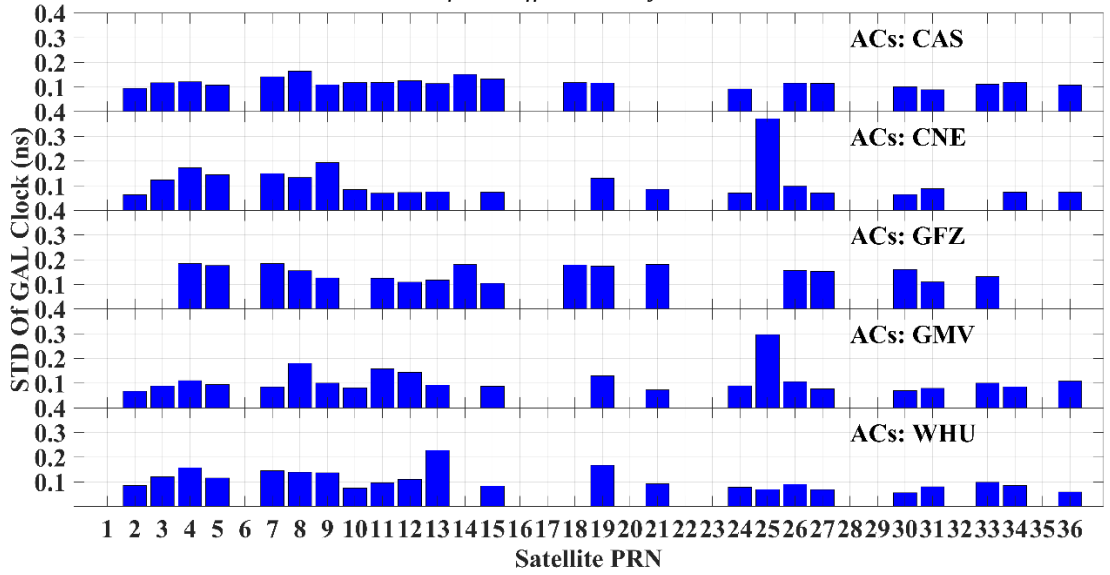

Figure 7

Precision of the real-time BDS MEO satellite clock errors from different analysis centers

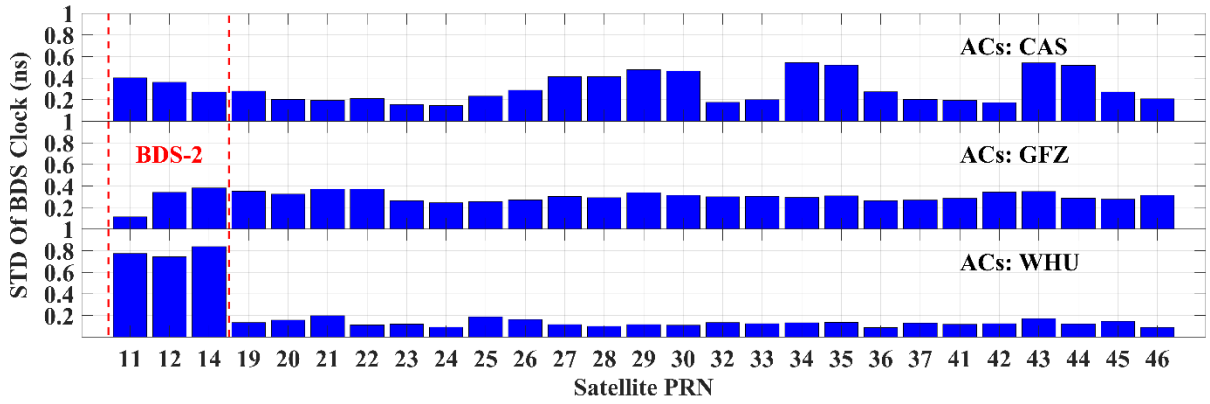

Table 4 lists the averaged STD of the satellite clock errors for all satellites in each constellation. The CNE and GMV GPS satellite clock errors have an STD below 0.1 ns. The GPS and Galileo satellite clock errors for all tested real-time products are below 0.16 ns. The BDS MEO satellite clock errors are generally twofold, around 0.3 ns.

Table 4

Averaged STD of the real-time satellite clock errors for GPS, Galileo and BDS MEO satellites

ACs	GPS (ns)	GAL (ns)	BDS MEO (ns)
CAS	0.1489	0.1187	0.3351
CNE	0.0937	0.1316	/
GFZ	0.1553	0.1531	0.3056
GMV	0.0905	0.1192	/
WHU	0.1134	0.1133	0.2905

3.3. SISRE of GNSS satellites to LEO satellites

As mentioned in Section 2.2, for ground users, the SISRE describes the combined GNSS satellite clock and orbital errors projected to the Earth. For LEO satellites, the projection coefficients vary slightly due to their higher altitudes than users on the Earth's surface.

Table 5 shows the averaged SISRE of various real-time GNSS products for both ground users and LEO satellites at different altitudes. The average SISRE of the GPS and Galileo real-time satellite products is generally at a few centimeters to sub-dm level, with CNE performing the best at 2.6 cm and 3.9 cm for GPS and Galileo, respectively. The SISREs of the GPS and Galileo satellites are generally at a similar level. Among all the BDS MEO products, WHU performed the best, with an average SISRE of about 1.05 dm. From Table 5, it can also be observed that the GNSS SISRE increases slightly with the user altitudes in most cases. This is caused by the slightly varying projection coefficients (see Table 1). As explained before, a shorterned distance between the GNSS satellites and the user would lead to larger contributions of the along-track and cross-track components, i.e., ω_{TA}. Here, the slightly increasing ω_{TA} leads to a larger role of the along-track and cross-track orbital errors when calculating the SISRE. As shown in Table 3, the along-track orbital errors of the GNSS satellites are mostly larger than those in the other two directions. As such, the SISRE in Table 5 increases correspondingly with the LEO satellite altitudes. In summary, the CNES real-time products performe the best for GPS and Galileo among all tested products, while for BDS MEO, WHU delivered the best performance.

Table 5

Average values of the SISRE of the real-time GPS, Galileo and BDS MEO satellite products to ground users (0 km) and LEO satellites at different altitudes

Acs		CAS	CNE	GFZ	GMV	WHU
GPS (m)	**0 km**	/	0.0261	0.0775	0.0391	0.0516
	500km		0.0262	0.0776	0.0391	0.0517
	1000km		0.0264	0.0777	0.0391	0.0517
	1500km		0.0266	0.0778	0.0391	0.0518
Galileo (m)	**0 km**	0.0623	0.0393	0.0766	0.0607	0.0504
	500km	0.0625	0.0395	0.0770	0.0607	0.0504
	1000km	0.0627	0.0397	0.0774	0.0607	0.0505
	1500km	0.0629	0.0400	0.0778	0.0607	0.0506
BDS MEO (m)	**0 km**	0.2063	/	0.1129	/	0.1057
	500km	0.2060		0.1131		0.1059
	1000km	0.2056		0.1132		0.1060
	1500km	0.2053		0.1133		0.1062

3.4. LEO satellite POD using real-time GNSS products

As a validation of the SISRE, real-time GNSS products of two different days from June 2023 are used to perform the LEO satellite POD for the satellite Sentinel-6A in the reduced-dynamic mode, which uses onboard collected GNSS observations to improve/estimate varous orbital dynamic parameters (Allahvirdi-Zadeh et al., 2021b). Dual-frequency phase and code observations tracked onboard the LEO satellite are used for the POD. The LEO satellite orbits are compared with the reference orbits provided by the Copernicus POD service (CSPDH, 2023). For comparison, the POD results using the COM final products are also given. The LEO satellite Orbital User Range Error (OURE), denoted as $\sigma_{\mathrm{L,OURE}}$, is computed here as the projection of the LEO satellite orbital errors to the Earth in an average sense:

$$\sigma_{\mathrm{L,OURE}} = \sqrt{\omega_{\mathrm{L,R}}^2 \sigma_{\mathrm{L,R}}^2 + \omega_{\mathrm{L,TA}}^2 \left(\sigma_{\mathrm{L,T}}^2 + \sigma_{\mathrm{L,A}}^2\right)} \tag{10}$$

where $\sigma_{\mathrm{L,R}}$, $\sigma_{\mathrm{L,T}}$ and $\sigma_{\mathrm{L,A}}$ represents the RMS of the radial, along-track and cross-track LEO satellite orbital errors. The projection coefficients $\omega_{\mathrm{L,R}}$ and $\omega_{\mathrm{L,TA}}$ are about 0.64 and 0.54, respectively, for Sentinel-6A flying at around 1300 km.

Table 6 shows, for example, the batch least-squares reduced-dynamic LEO POD results using different GPS real-time products. It can be observed that all tested real-time products can deliver high-accuracy LEO POD results in near-real-time. Compared with the COM final products that gave a $\sigma_{\mathrm{L,OURE}}$ below 2 cm, the real-time products exhibit only slightly worse POD performance, i.e., with a $\sigma_{\mathrm{L,OURE}}$ below or around 3 cm. This corresponds to their good SISRE performances for GPS satellites in Section 3.3.

Table 6

RMS of the LEO satellite orbital errors for Sentinel-6A using different real-time GNSS products

ACs	System	June 11, 2023 (m)				June 2, 2023 (m)			
		$\sigma_{\mathrm{L,R}}$	$\sigma_{\mathrm{L,T}}$	$\sigma_{\mathrm{L,A}}$	$\sigma_{\mathrm{L,OURE}}$	$\sigma_{\mathrm{L,R}}$	$\sigma_{\mathrm{L,T}}$	$\sigma_{\mathrm{L,A}}$	$\sigma_{\mathrm{L,OURE}}$
COM	GE	0.0111	0.0184	0.0249	0.0183	0.0128	0.0214	0.0143	0.0162
CNE	G	0.0244	0.0366	0.0215	0.0278	/			
WHU	G	0.0233	0.0387	0.0290	0.0302	0.0223	0.0354	0.0294	0.0288
GMV	G	0.0194	0.0341	0.0506	0.0354	/			
CAS	G	/				0.0192	0.0312	0.0369	0.0290
GFZ	G					0.0261	0.0410	0.0300	0.0323

3.5. Overbounding values of the combined satellite orbital and clock errors

In addition to the SISRE, the integrity of the real-time GNSS satellite products is essential for integrity monitoring of the LEO satellite POD and clock determination. As such, this Section also provides an analysis of the integrity of the investigated real-time GNSS products. The overbounding standard deviations and mean values (i.e. considered as biases) of the combined GNSS satellite orbital and clock errors are computed for different constellations using the Stanford two-step method as mentioned in Section 2.3.

Table 7 lists the overbounding standard deviations ($\breve{\sigma}$) and mean values ($\breve{m}$) of the combined multi-GNSS satellite orbital and clock errors for ground users and LEO satellites at different altitudes. The overbounding values for GPS and Galileo satellites are below 1 dm, and for BDS MEO satellites they are slightly larger, i.e., ranging from sub-dm to about 2 dm. The products from CNES provided the smallest overbounding values for GPS and Galileo, and the WHU products delivered the smallest overbounding values for the BDS MEO satellite.

Table 7

Overbounding values of the combined satellite orbital and clock errors

ACs		GPS (m)		GAL (m)		BDS MEO (m)	
		$\breve{\sigma}_{GPS}$	$\breve{m}_{GPS}$	$\breve{\sigma}_{GAL}$	$\breve{m}_{GAL}$	$\breve{\sigma}_{BDS}$	$\breve{m}_{BDS}$
CAS	**0 km**	/		0.0649	0.0356	0.2398	0.1494
	500km			0.0643	0.0365	0.2351	0.1509
	1000km			0.0632	0.0372	0.2295	0.1534
	1500km			0.0634	0.0377	0.2285	0.1550
CNE	**0 km**	0.0357	0.0182	0.0406	0.0297	/	
	500km	0.0301	0.0186	0.0419	0.0305		
	1000km	0.0308	0.0190	0.0422	0.0313		
	1500km	0.0310	0.0196	0.0423	0.0318		
GFZ	**0 km**	0.0824	0.0709	0.0787	0.0889	0.1598	0.0829
	500km	0.0817	0.0726	0.0793	0.0910	0.1597	0.0842
	1000km	0.0827	0.0736	0.0794	0.0930	0.1584	0.0863
	1500km	0.0819	0.0752	0.0803	0.0957	0.1610	0.0870
GMV	**0 km**	0.0608	0.0302	0.0485	0.0345	/	
	500km	0.0604	0.0305	0.0487	0.0351		
	1000km	0.0601	0.0309	0.0502	0.0357		
	1500km	0.0618	0.0315	0.0507	0.0364		
WHU	**0 km**	0.0564	0.0379	0.0641	0.0347	0.1170	0.0697
	500km	0.0559	0.0387	0.0665	0.0350	0.1154	0.0714
	1000km	0.0561	0.0392	0.0631	0.0357	0.1155	0.0727
	1500km	0.0559	0.0400	0.0610	0.0366	0.1188	0.0739

4. CONCLUSIONS

LEO satellites are frequently discussed to enhance GNSS PNT services in recent years. A prerequisite for LEO augmentation is the good quality of the real-time LEO orbital and clock products, and indirectly, the high precision of real-time GNSS products used for its POD and clock determination. In this study, the multi-GNSS satellite orbital accuracy and clock precision of real-time products from different analysis centers are analyzed based on one week of data. The SISREs of different GNSS constellations are calculated for ground users and LEO satellites at different altitudes. Using the real-time GNSS products, LEO satellite POD results are given for the purpose of validation. The overbounding standard deviations and mean values of combined satellite orbital and clock errors were computed using the two-step method. The major conclusions are given as follows:

- In general, the GPS and Galileo real-time products deliver similar accuracy and availability, while those of the BDS MEO satellites are generally a bit worse. In the case of GPS and Galileo, GMV provided the best orbital accuracy and clock precision, with orbital accuracy of about 5 cm and clock precision of about 0.1 ns. WHU provided the best BDS MEO products with orbital accuracy at around 1.2 dm and clock precision at 0.29 ns, respectively.

- For ground users and LEO satellites at different altitudes, the SISRE of the GPS and GAL real-time products ranges from centimeters to sub-dm level, with CNES products exhibiting the best performance of about 2.6 cm for GPS and 3.9 cm for Galileo. In the case of BDS MEO, WHU demonstrated the best performance with SISRE of about 10 to 11 cm. In most cases, the SISRE tends to rise when increasing the user altitude.

- Concerning the overbounding values of the combined GNSS satellite orbital and clock errors to be used for estimating integrity of the POD solution, the CNES products gave the best performance for GPS and Galileo with an overbonding standard deviation of about 3-4 cm and an overbounding mean value of about 2-3 cm, respectively. For BDS MEO satellites, WHU delivered the smallest overbounding standard deviation of about 11-12 cm and the overbounding mean value of around 7 cm.

- The best performance of the real-time GPS/Galileo orbital and clock products was found to be provided by GMV, while the smallest SISRE was provided by the CNES products. This suggests that the accuracy of the combined projection errors of the orbits and clocks, which is of main interest, might differ from those of the indvidual orbital and clock products.

ACKNOWLEDGEMENTS

This work is funded by the National Time Service Center, Chinese Academy of Sciences (CAS) (No. E167SC14), the National Natural Science Foundation of China (No. 12073034) and the Australian Research Council—discovery project (No. DP 190102444). We also acknowledge the support of the international GNSS monitoring and assessment system (iGMAS) at the National Time Service Center, and the National Space Science Data Center, National Science & Technology Infrastructure of China (http://www.nssdc.ac.cn).

REFERENCES

Allahvirdi-Zadeh, A., Wang, K., & El-Mowafy, A. (2021a). POD of small LEO satellites based on precise real-time MADOCA and SBAS-aided PPP corrections. *GPS Solutions*, *25*, 31. https://doi.org/10.1007/s10291-020-01078-8

Allahvirdi-Zadeh, A., Wang, K., & El-Mowafy, A. (2021b). Precise orbit determination of LEO satellites based on undifferenced GNSS observations, J. of Surveying Engineering, https://doi.org/10.1061/(ASCE)SU.1943-5428.0000382

Blanch, J., Walter, T., & Enge, P. (2019). Gaussian Bounds of Sample Distributions for Integrity Analysis. *IEEE Transactions on Aerospace and Electronic Systems*, *55*(4), 1806-1815. https://doi.org/10.1109/TAES.2018.2876583

Chen, L., Jiao, W., Huang, X., Geng, C., Ai, L., Lu, L., & Hu, Z. (2013). Study on signal-in-space errors calculation method and statistical characterization of BeiDou navigation satellite system. In Proceedings of the China Satellite Navigation Conference (CSNC) 2013; Sun J, Jiao W, Wu H, Shi C, Eds.; Lecture Notes in Electrical Engineering, Volume 243; Springer: Berlin, Heidelberg, Germany.

CSPDH (2023). Copernicus Sentinels POD Data Hub. Copernicus Open Access Hub, Europen Space Agency. Accessed on January 24, 2023 at https://scihub.copernicus.eu/gnss

Ding, W., Tan, B., Chen, Y., Teferle, F. N., & Yuan, Y. (2018). Evaluation of a regional real-time precise positioning system based on GPS/BeiDou observations in Australia. *Advances in Space Research*, *61*(3), 951-961. https://doi.org/10.1016/j.asr.2017.11.009

Ge, H., Li, B., Ge, M., Zang, N., Nie, L., Shen, Y., & Schuh, H. (2018). Initial assessment of precise point positioning with LEO enhanced global navigation satellite systems (LeGNSS). *Remote Sensing*, *10*(7), 984. https://doi.org/10.3390/rs10070984

GPS World Staff (2017). PNT Roundup: Iridium constellation provides low-Earth orbit satnav service. GPS World, January 12, 2017. https://www.gpsworld.com/iridium-constellation-provides-low-earth-orbit-satnav-service/#:~:text=Based%20on%20the%20low%2DEarth,buildings%20and%20other%20difficult%20locations.

GMV (2023). GMV Aerospace & Defence SAU (iafastro.org). International Astronomical Federation. Accessed on 14 October 2023 on GMV Aerospace & Defence SAU (iafastro.org)

Guo, L., Zhao, Q., Xu, X., Tao, J., Zhang, Q., Qu, Z., Chen, G., & Wang, C. (2018). Real-time orbit and clock products at Wuhan University to support Multi-GNSS applications. *IGS Workshop*, Wuhan, China, 29 October – 2 Novermber, 2018

Hauschild, A., Tegedor, J., Montenbruck, O., Visser, H., & Markgraf, M. (2016) Precise onboard orbit determination for LEO satellites with real-time orbit and clock corrections. *In Proc. ION GNSS+ 2016*, Institute of Navigation, Portland, Oregon, USA, September 12-16, 3715-3723.

Hauschild, A., Montenbruck, O., Steigenberger, P., Martini, I., & Fernandez-Hernandez, I. (2022). Orbit determination of Sentinel-6A using the Galileo high accuracy service test signal. *GPS Solutions*, *26*, 120. https://doi.org/10.1007/s10291-022-01312-5

Heng, L., Gao, GX., Walter, T., Enge, P. (2011) Statistical characterization of GPS signal-in-space errors. In Proc. *2011 ION ITM*, San Diego, CA, USA, 24–26 January 2011, pp 312–319

Kazmierski, K., Sośnica, K., Hadas, T. (2018) Quality assessment of multi-GNSS orbits and clocks for real-time precise point positioning. *GPS Solutions*, *22*(11), 11. https://doi.org/10.1007/s10291-017-0678-6

Li, B., Ge, H., Bu, Y., Zheng, Y., & Yuan, L. (2022). Comprehensive assessment of real-time precise products from IGS analysis centers. *Satellite Navigation*, 3(1), 12. https://doi.org/10.1186/s43020-022-00074-2

Lawrence, D., Cobb, H. S., Gutt, G., O'Connor, M., Reid, T. G. R., Walter T., & Whelan, D. (2017). Innovation: Navigation from LEO. *GPS World*, June 30, 2017. https://www.gpsworld.com/innovation-navigation-from-leo/

Li, X., Ma, F., Li, X., Lv, H., Bian, L., Jiang, Z., & Zhang, X. (2018a). LEO constellation-augmented multi-GNSS for rapid PPP convergence. *Journal of Geodesy*, *93*, 749-764. https://doi.org/10.1007/s00190-018-1195-2

Lyard, F., Lefevre, F., Letellier, T., & Francis, O. (2006). Modelling the global ocean tides: Modern insights from FES2004. *Ocean Dyn.*, *56*, 394–415.

Männel, B., Brandt, A., Nischan, T., Brack, A., Sakic, P., & Bradke, M. (2020). GFZ rapid product series for the IGS. GFZ Data Services. https://doi.org/10.5880/GFZ.1.1.2020.003

Michalak, G., Glaser, S., Neumayer, K. H., König, R. (2021). Precise orbit and Earth parameter determination supported by LEO satellites, inter-satellite links and synchronized clocks of a future GNSS. *Advances in Space Research, 12*, 4753–4782. https://doi.org/10.1016/j.asr.2021.03.008

Montenbruck, O., & Gill, E. (2000). Around the world in a hundred minutes. *Satellite orbits, 1st ed.;* Springer: Berlin, Heidelberg, Germany, 1–13.

Montenbruck, O., Hauschild, A., Andres, Y., von Engeln, A., & Marquardt, C. (2013). (Near-) real-time orbit determination for GNSS radio occultation processing. *GPS Solutions*, *17*, 199-209. https://doi.org/10.1007/s10291-012-0271-y

Montenbruck, O., Steigenberger, P., & Hauschild, A. (2018). Multi-GNSS signal-in-space range error assessment – Methodology and results. *Advances in Space Research*, *61*(12), 3020-3038. https://doi.org/10.1016/j.asr.2018.03.041

Rife, J., Pullen, S., Enge, P., Pervan, B. (2006) Paired overbounding for nonideal LAAS and WAAS error distributions. *IEEE Transactions on Aerospace and Electronic Systems*, 42(4):1386–1395. https://doi.org/10.1109/TAES.2006.314579

Reid, T. G. R., Neish, A. M., Walter, T., & Enge, P. K. (2018). Broadband LEO constellations for navigation. *Navigation, Journal of the Institute of Navigation*, *65*(2), 205–220. https://doi.org/10.1002/navi.234

Reid, T., Banville, S., Chan, B., Gunning, K., Manning, B., Marathe, T., Neish, A., Perkins, A., & Sibois, A. (2022). PULSAR: A New Generation of Commercial Satellite Navigation. *ION GNSS+ 2022*, September 11-15, 2023, Denver, Colorado, USA

Schaer, S., Villiger, A., Arnold, D., Dach, R., Prange, L., & Jäggi, A. (2021). The CODE ambiguity-fixed clock and phase bias analysis products: Generation, properties, and performance. *Journal of Geodesy*, *95*(7), 1–25.

Villiger, A., Schaer, S., Dach, R., Prange, L., Sušnik, A., & Jäggi, A. (2019). Determination of GNSS pseudo-absolute code biases and their long-term combination. *Journal of Geodesy*, *93*(9):1487–1500

Wang, K., El-Mowafy, A., Rizos, C. (2021) Integrity monitoring for precise orbit determination of LEO satellites. *GPS Solutions*, 26(1), 32. https://doi.org/10.1007/s10291-021-01200-4

Wang, K., El-Mowafy, A., Yang, X. (2022) URE and URA for predicted LEO satellite orbits at different altitudes. *Advances in Space Research*, 70(8), 2412-2423. https://doi.org/10.1016/j.asr.2022.08.039

Wang, K., El-Mowafy, A., Wang, W., Yang, L., & Yang, X. (2022). Integrity Monitoring of PPP-RTK Positioning; Part II: LEO Augmentation. *Remote Sensing, 14*(7), 1599. https://doi.org/10.3390/rs14071599

Weber, G., & Mervart, L. (2007). The BKG ntrip client (BNC). In *Report on EUREF symposium*.

Yang, L. (2019). The Centispace-1: A LEO Satellite-Based Augmentation System. *The 14th Meeting of the International Committee on Global Navigation Satellite Systems*, Bengaluru, India, 8 - 13 December 2019

Yu, C., Zhang, Y., Chen, J., Chen, Q., Xu, K., & Wang, B. (2023). Performance Assessment of Multi-GNSS Real-Time Products from Various Analysis Centers. *Remote Sensing*, 15(1), 1-40. https://doi.org/10.3390/rs15010140